Power rating based on two different spectroheliometers with lattice-matched (LM) and upright metamorphic (UMM) component solar cells

César Domínguez, Rebeca Herrero, Rubén Núñez, Ignacio Antón, Gabriel Sala, and Emilio Agudo

Citation: AIP Conference Proceedings **1766**, 100002 (2016); doi: 10.1063/1.4962117
View online: http://dx.doi.org/10.1063/1.4962117
View Table of Contents: http://scitation.aip.org/content/aip/proceeding/aipcp/1766?ver=pdfcov
Published by the AIP Publishing

Power Rating Based on Two Different Spectroheliometers with Lattice-Matched (LM) and Upright Metamorphic (UMM) Component Solar Cells

César Domínguez[1, a)], Rebeca Herrero[1], Rubén Núñez[1], Ignacio Antón[1], Gabriel Sala[1] and Emilio Agudo[2]

[1]*Instituto de Energía Solar, Universidad Politécnica de Madrid. Madrid, Spain.*
[2]*Solar Added Value, S.L. Madrid, Spain*

[a)]Corresponding author: cesardd@ies-def.upm.es

Abstract. Synthetic and empirical data have been used to explore the influence of spectral mismatch between MJ cell technologies on outdoor CPV module rating uncertainty. Calibration biases are attenuated by tightly filtering spectral conditions to a spectral matching ratio (SMR) of 1 ± 2.5%. The sensitivity of calibrated current to spectral deviations greatly depends on the direction and distribution of the deviations on the SMR space.

INTRODUCTION

The committee draft version (CDV) of the norm IEC 62670-3 on power rating of CPV modules has recently been voted and will be probably published in 2016. Its main objective is the definition of reproducible procedures for assuring indoor and outdoor power rating with a low uncertainty. It takes from the experience cumulated through the round robin campaigns carried out in the last years, in which 10 different labs worldwide have contributed with their experience in outdoor CPV rating [1–5]. The key idea to assure repeatability is to control measurement conditions and report nominal power for a set of standard conditions. These are not necessarily achieved during measurements, but the I-V curves acquired are translated towards standard conditions through some well-documented methods. However, in regard of spectral conditions, to which CPV systems employing multijunction (MJ) cells are very sensitive, the norm does not suggest corrections but tightly filtering measurements to those obtained under a solar spectrum very similar to the AM1.5D standard distribution. Deviations from the reference spectrum affect the relationship between module current and direct normal irradiance (DNI) because of current mismatch losses between MJ subcells, which has a direct impact on the definition of the reference short-circuit current I_{SC} (e.g. as in the calibration of a mono-module) and the rated power. The norm recommends that spectral conditions evaluated by comparing the relative weight of different spectral bands under both the current spectrum and the reference AM1.5D. The bands should be those defined by the bandgaps of the MJ solar cell in the module under test. This comparison is quantified through the so-called spectral matching ratio (SMR), which divides the current ratio between any two subcells under the current spectrum, by their ratio under reference spectrum [7]:

$$\mathrm{SMR}_{\mathrm{subcell_j}}^{\mathrm{subcell_i}}(\mathrm{E}(\lambda)) = \frac{\mathrm{J_{L,ratio}}_{\mathrm{subcell_j}}^{\mathrm{subcell_i}}(\mathrm{E}(\lambda))}{\mathrm{J_{L,ratio}}_{\mathrm{subcell}_j}^{\mathrm{subcell_i}}(AM1.5D)} = \frac{\frac{\mathrm{I_{L,subcell_i}}_{\mathrm{E}(\lambda)}}{\mathrm{I_{L,subcell_j}}_{\mathrm{E}(\lambda)}}}{\frac{\mathrm{I_{L,subcell_i}}_{AM1.5D}}{\mathrm{I_{L,subcell_j}}_{\mathrm{AM1.5D}}}} \quad (1)$$

where $\mathrm{I_{L,subcell_i}}_{\mathrm{E}(\lambda)}$ represents the photocurrent of subcell i when illuminated with a particular spectral irradiance distribution $E(\lambda)$ and $\mathrm{I_{L,subcell_i}}_{AM1.5D}$ stands for the photocurent of subcell i under the reference spectrum. The SMR can be given for any two subcells, but for three subcells there are only two unique values. Considering, for example,

12th International Conference on Concentrator Photovoltaic Systems (CPV-12)
AIP Conf. Proc. 1766, 100002-1–100002-6; doi: 10.1063/1.4962117
Published by AIP Publishing. 978-0-7354-1424-2/$30.00

a germanium-based lattice-matched triple junction (3J) solar cell and its corresponding component cells, three spectral indexes can be defined: SMR_{mid}^{top}, SMR_{bot}^{top} , SMR_{bot}^{mid} where the scripts *top*, *mid* and *bot* stand for the top GaInP subcell, the middle GaInAs subcell and the bottom Ge subcell, respectively. In the case of triple junction cells, only two of these SMR values are unique, so SMR_{mid}^{top} and SMR_{bot}^{mid} form a set of indexes that fully characterize the spectral irradiance for that particular MJ solar cell technology. Conditions of $SMR_{mid}^{top} = SMR_{bot}^{mid} = 1$ indicate effective AM1.5D spectrum. Instruments like a *spectroheliometer* for the measurement of DNI using component or 'isotype' cells should be used. In the absence of outdoor component cells, the norm recommends the use of spectroradiometers for measuring the spectrum of direct light and then integrating the spectrum in the spectral bands of interest (those of the MJ in the device under test) to calculate the relevant SMR values.

Outdoor Power Rating Biases

The IEC 62670-3 draft proposes a tolerance of 2.5% around SMR = 1 for all subcell pairs. This is a trade-off for between low spectral bias and a relevant number of samples. The probability of achieving these valid spectral conditions depends on the atmospheric conditions and solar height. In particular, $SMR_{mid}^{top} = 1$ is usually achieved twice per day in clear days outside winter for medium latitudes, although this can be influenced by the amount of aerosols in the atmosphere. Regarding middle-to-bottom SMR, which is mainly a function of the precipitable water (PW) and aerosols content of the atmosphere, achieving reference conditions is strongly influenced by local conditions. Under stable atmospheric conditions, it is common that the value of PW doesn't change much so it is expected that several days are needed for achieving the SMR = 1 crossing.

Due to this limited variability of spectral conditions, an outdoor measurement campaign can end up with a limited amount of valid data, which may increase the uncertainty of the resulting power rating. Possible calibration biases depend on the characteristics of the filtered data subset, even with a narrow spectral tolerance as it is specified by the IEC standard. In this work, we explore the conditions that allow accurate calibrations for reduced data subsets linked to measurement campaigns with few valid days.

Another possible calibration bias may appear when the solar cell architectures of the spectroheliometer (component cells) and the device under test (DUT) differ, which introduces a spectral mismatch due to the different shape or bounds of their spectral responses. Different types of component cells calibrated under AM1.5D may quantify different SMR values under non-reference spectra [8]. Furthermore, the norm allows using a generic set of component cells with the bandgaps of Ge-based lattice matched triple-junction cells (LM-Ge) for measuring SMR, which may differ from the cell in the module under test. We investigate here the uncertainties or calibration biases that this spectral mismatch may introduce.

EXPERIMENTAL

Since spectral variations mainly affect the linearity between short-circuit current and DNI, our approach in this work is to investigate the variations in the I_{SC} normalized to DNI as a function of spectral conditions. We establish a calibrated value of this normalized current, I_{CAL} as the average of a large set of long-term measurements filtered to spectral conditions strictly close to AM1.5D. This calibration value is also used in indoor rating procedures for identifying reference DNI with a CPV reference sensor and therefore it has a direct impact on the rated power indoors as well.

In this investigation we use both a synthetic dataset of spectral conditions and an outdoor measurement campaign of CPV modules and spectroheliometers carried out at the Instituto de Energía Solar (IES-UPM) facilities in Madrid, Spain in the spring of 2016. Firstly, the 2014 annual series of DNI spectra for Madrid is synthesized with SMARTS using atmospheric data from the local AERONET station (15 min. resolution typ.). The photogenerated current of each subcell in 5 different types of state-of-the-art MJ cell architectures is calculated for every spectrum by integrating their spectral response multiplied by the instantaneous spectral irradiance. The pair of $SMR_{mid}^{top}, SMR_{bot}^{mid}$ values is calculated for each cell technology in order to study deviations between them. The electrical response of each cell (I_{SC}) is calculated as the minimum of the three subcell currents, which is then normalized by the DNI obtained by integrating the synthetic solar spectrum alone. The 5 types of triple-junction solar cell technologies investigated are summarized in FIGURE 1: Ge-based lattice-matched (LM-Ge), upright metamorphic (of two different types, UMM-A and UMM-B), inverted metamorphic and dilute-nitrides lattice-matched (LM-DN) solar cells. IMM and LN-DN cells use bottom subcells without a great current excess because of its higher bandgap. The

main difference in the UMM-A with respect to the UMM-B is that the latter takes the atmospheric water vapor absorption gap within the spectral response of the middle subcell, which has significant consequences in the SMR_{bot}^{mid} calculations.

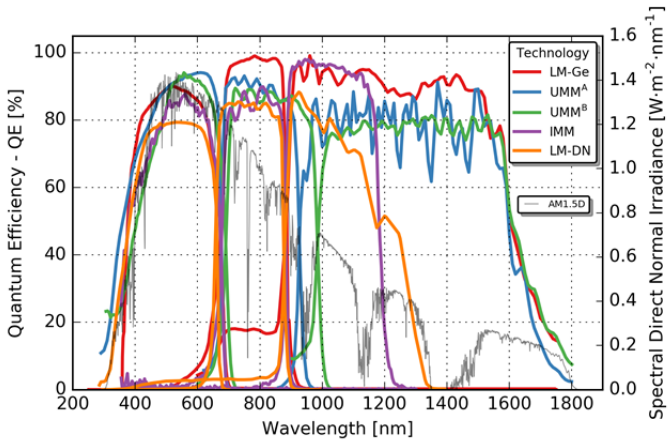

FIGURE 1. Spectral response (as external quantum efficiency) of the 5 types of solar cells investigated, together with the ASTM G173-03 reference spectral irradiance distribution AM1.5D (in gray).

Using the complete annual series of spectra under $SMR_{mid}^{top} = SMR_{bot}^{mid} = 1$, the calibrated value of the normalized current, I_{CAL} is obtained. This value will be compared with the averages extracted for subsets of data for particular days $\overline{I_{CAL}}$ in order to investigate calibration biases: $Calibration\ Bias = (\overline{I_{CAL}} - I_{CAL})/I_{CAL} \cdot 100(\%)$.

The validity of the conclusions obtained with the synthetic data is explored empirically through an outdoor measurement campaign during the spring of 2016. The I-V curves from two different CPV modules installed on a precision two-axis tracker were monitored: one employs LM-Ge type MJ cells, while the other uses UMM-A cells. The spectral conditions were continuously monitored using two ICU-3J35 spectroheliometers from Solar Added Value at the IES-UPM meteo station, one with component or 'isotype' cells equivalent to the LM-Ge MJ cell and the other with UMM-A component cells.

RESULTS AND DISCUSSION

For the convenient display of the results, we plot each data point of the I_{SC} normalized by the DNI in false color over the two-dimensional space created by the SMR_{mid}^{top} and SMR_{bot}^{mid} axes, as in FIGURE 2. In this space, the (1,1) coordinate is the reference spectrum AM1.5D and three different spectral tolerance values around AM1.5D are shown for reference: ±10% (blue square), ±5% (green) and ±2.5% (red), the latter being the limits recommended in the draft of the norm. Rather than the absolute I_{SC}/DNI ratio for each data point, we plot its variation in percentage with respect to the calibration value under reference conditions, I_{CAL}. FIGURE 2(a) shows the 2014 annual dataset of I_{SC}/DNI values (reduced to the $SMR_{mid}^{top} > 0.8$ bound shown in the figure, which corresponds to a very high air mass and low DNI) calculated for the LM-Ge cell architecture using the synthesized spectra from SMARTS, which reveals the large variability of air mass and atmospheric conditions found throughout the year in Madrid in clear sky days. Data points correspond to the AERONET database timestamps. Some ideas are worth being drawn from the graph now. First, note that spectral losses smoothly correlate with SMR values. However, the sensitivity to spectral variations depend on the direction followed across the two-dimensional SMR space. The yellow arrow approximately shows the direction with the greatest rate of change of the I_{SC}/DNI ratio starting from the (1,1) coordinate, i.e. AM1.5D conditions. On the contrary, the blue arrow shows variations in the spectral conditions for which the normalized current stays approximately constant, i.e. an iso-calibration contour line. If one was to have very few days of valid data close to but not exactly AM1.5D, measurements across these iso-calibration bands would be preferred for assuring low calibration biases. Furthermore, balanced datasets across two symmetrical quadrants (i.e. having crossed unit SMR in both axes) may introduce lower calibration biases than unbalanced datasets (i.e. having more measurement in one quadrant of the SMR space than in the (diagonal) opposite one), just because positive and negative errors will be compensated when taking their average. As a final remark, the largest

normalized currents (warm color dots) are found in the first 'quadrant', i.e. $(SMR_{mid}^{top}, SMR_{bot}^{mid}) > 1$, where the current in the bottom subcell is reduced without affecting I_{SC} because it has a substantial excess of current under AM1.5D. The characteristics found for this synthetic series have been validated experimentally using a spectro-heliometer with a set of component cells of the same type of LM-Ge triple-junction cell. The map obtained for the 2014 year at the IES-UPM meteo station (at the same campus as the Madrid AERONET station) is shown in FIGURE 2(b), which displays very similar trends, although further filling the SMR space towards higher SMR_{mid}^{top} values.

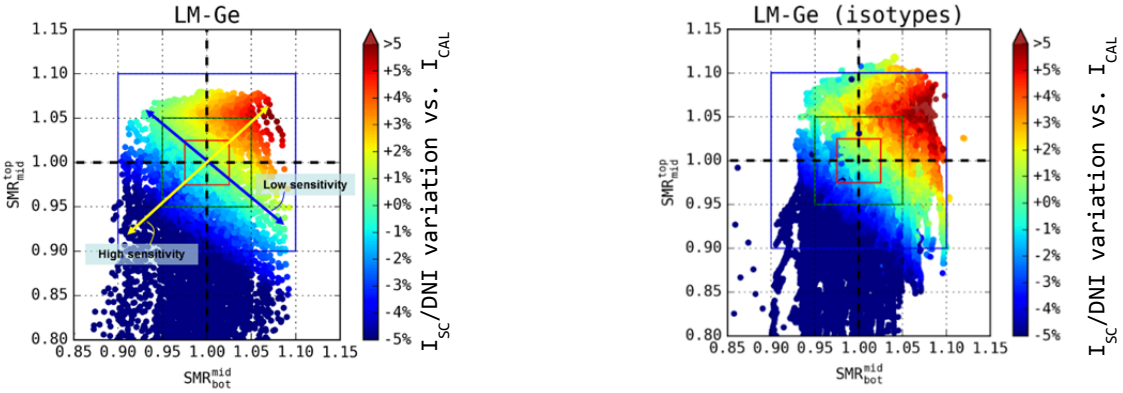

FIGURE 2. Variations of the short-circuit current normalized to DNI in clear sky conditions for the whole 2014 year in Madrid, both synthesized (a) or actually measured (b) at the IES-UPM meteo station.

FIGURE 3 shows the effect of the same 2014 annual series of spectra on the other 4 types of MJ cell architectures. All maps show a shape somewhat similar to a diamond, although shifted and clipped to different bounds. UMM-A and IMM solar cell maps appear shifted towards low SMR_{mid}^{top} values, which is explained by a larger excess in top subcell current. For the UMM-B cell, where the large spectrum valley due water absorption between 900 and 1000 nm is taken by the middle cell response rather than by the bottom as in the other cells, the map spans over a markedly narrower SMR_{bot}^{mid} range: it is a poorer indicator of spectral variations due to water vapor. It is interesting to think of these differences in shape as transformations of the two-dimensional space of spectral conditions for each type of cell, helping understand to which extent a particular set of component cells cannot unequivocally identify a particular effective spectrum. However, a positive outcome of the spectral sensitivity maps shown is that if we stick to the ±2.5% spectral tolerance limits recommended by the norm, the dispersion in the normalized current values is mostly below ±2%. As a reference, this value is lower than the uncertainty in the measurement of SMR.

In a real situation for a calibration laboratory, a short measurement campaign of several weeks might end up with only a few days of valid data following the tight filtering of the norm. If the resulting dataset is well balanced across both SMR dimensions around AM1.5D, the calibration bias will be small, as shown in FIGURE 4(a). However, unbalanced datasets as in FIGURE 4(b) may introduced significant calibration biases even after the spectral filtering of ±2.5% recommended in the norm. Still, unbalanced datasets might not introduced calibration biases if they are distributed over the iso-calibration bands or they are filtered to tighter bounds.

In the case that the module under test uses MJ cells for which the calibration laboratory does not have equivalent component cells, a calibration bias may appear due to the spectral mismatch between both technologies. In FIGURE 5(a) we show the actual SMR experienced by each cell technology after filtering with some LM-Ge component cells. The color lines define the bounds of the remaining data, and the marked point is the resulting average. As first remark, the encircled data are also within the appropriate bounds according to their own definition of SMR. Furthermore, the average calibration values are very close to each other. Then another valid day but with an unbalanced dataset (FIGURE 5(b)) shows regions further from each other, with means now up to 2% different. We can conclude that for most 3J cell architectures, the mismatch between DUT and component cells has little influence for this tight spectral filtering.

In the empirical investigations performed using two types of CPV modules (LM-Ge and UMM-A) at the IES-UPM rooftop, again the calibration biases found were low for the spectral mismatch between DUT and component cells, while significantly larger for poorly balanced datasets.

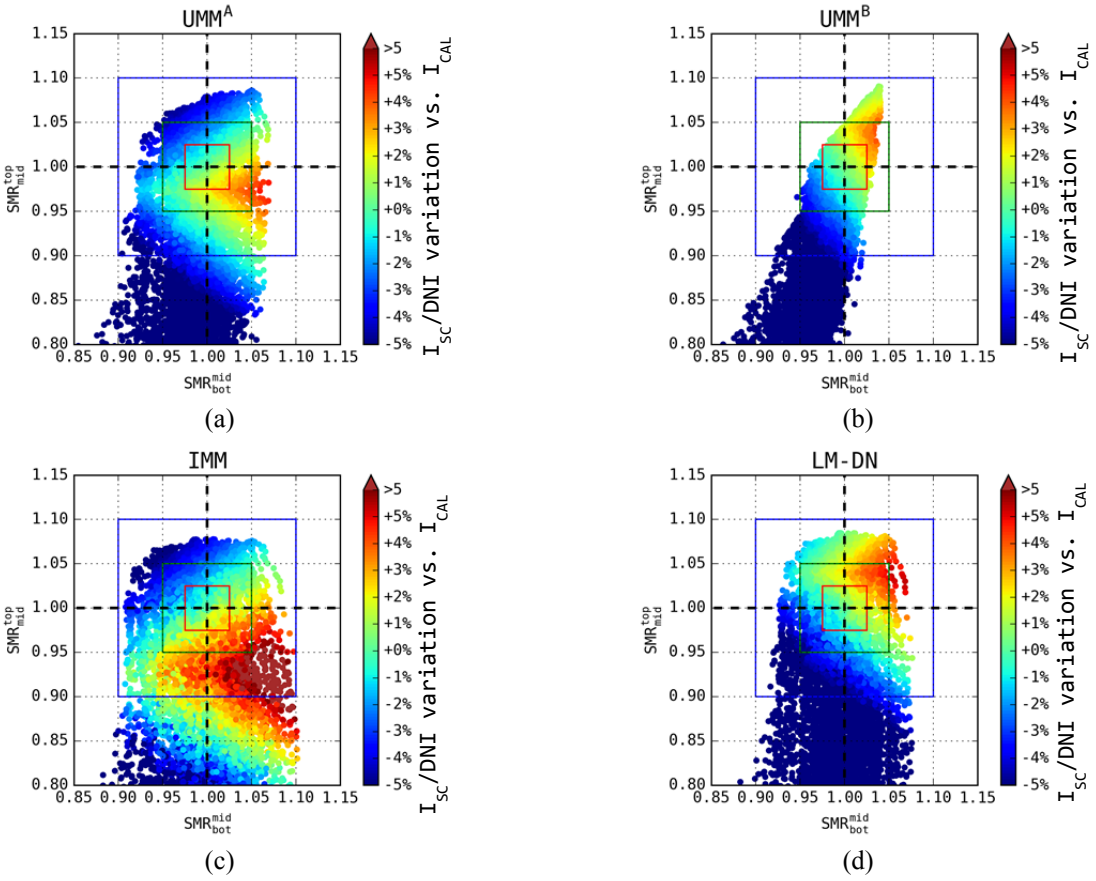

FIGURE 3. Spectral variations of the normalized current during 2014 in Madrid for the representative (a) UMM-A, (b) UMM-B, (c) IMM and (d) LM-DN multi-junction solar cells analyzed in this work.

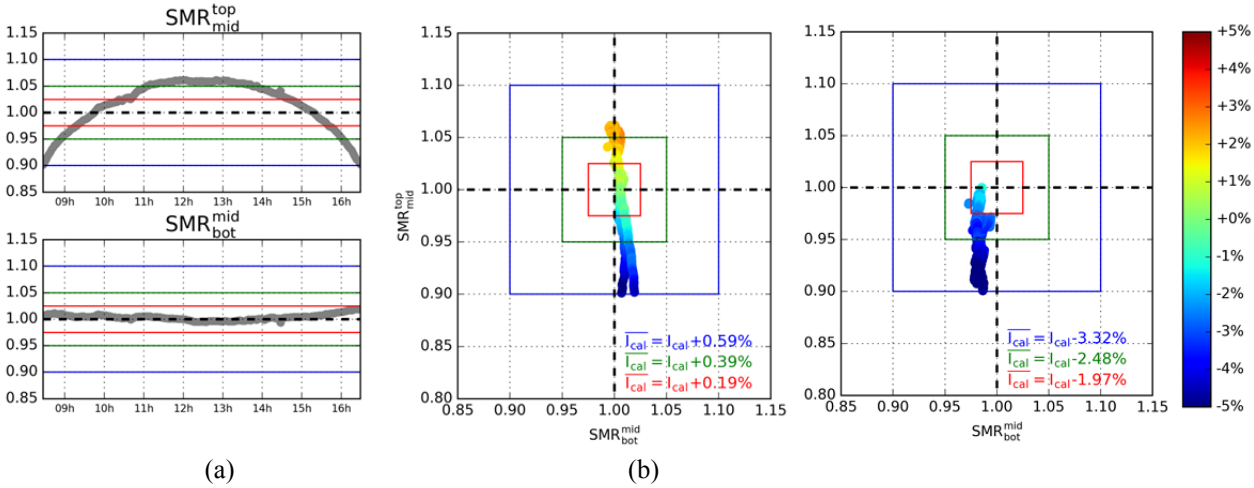

FIGURE 4. Spectral variations in both SMR indices throughout a single day (a), where the low variation of SMR(middle vs. bottom) under stable atmospheric conditions can be noted. This type of day yields a well-balanced data set (b) and a low calibration bias (0.19% for the ±2.5% filtering of the norm). However, unbalanced datasets as in (c) may introduced significant calibration biases even for the tightest spectral filtering.

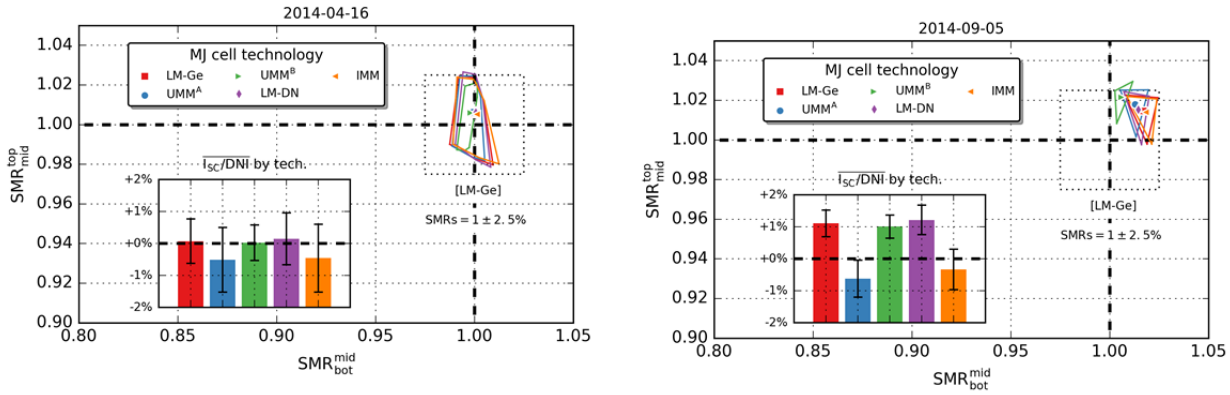

(a) (b)

FIGURE 5. Spectral conditions experienced in a well-balanced day (a) and a poorly balanced day (b) by each type of MJ cell after filtering with LM-Ge component cells following the norm draft procedure.

CONCLUSIONS

Synthetic and empirical data have been used to explore the influence of spectral mismatch between MJ cell technologies on rating uncertainty. The SMR measured using component cells allows for reproducible outdoor rating procedures with low uncertainty when filtering to narrow ±2.5%. The sensitivity of calibrated current to spectral deviations depends on the direction and distribution of the deviations on the SMR space. The errors introduced by the spectral mismatch between DUT and component cells are attenuated by using the spectral filter bounds defined by the IEC 62670-3 norm draft, for which SMR spaces are very close between technologies.

ACKNOWLEDGEMENTS

We acknowledge the financial support provided by the Comunidad de Madrid through the program MADRID-PV-CM (S2013/MAE2780) and by the European Union's Horizon 2020 within the project CPVMatch under grant agreement No 640873.

REFERENCES

1. I. Antón, D. Pachón, and G. Sala, in 19th Eur. Photovolt. Sol. Energy Conf. Exhib., edited by W.-M. a. ETA-Florence (París (Francia), 2004), pp. 2121–2124.
2. I. Antón, M. Martínez, F. Rubio, R. Núñez, R. Herrero, C. Domínguez, M. Victoria, S. Askins, and G. Sala, in AIP Conf. Proc. (AIP Publishing, 2012), pp. 331–335.
3. M. Muller, S. Kurtz, and J. Rodriguez, in AIP Conf. Proc. (AIP Publishing, 2013), pp. 125–128.
4. A. Datas, A.B.C. López, G.S. Pano, I.A. Hernandez, J.C.M. Dominguez, P.B. Gimenez, A.W. Bett, G. Siefer, N. Ekins-Daukes, F. Roca, C. Cancro, I. Luque-Heredia, W. Warmuth, M. Baudrit, Y. Okada, M. Sugiyama, Y. Hishikawa, T. Takamoto, K. Araki, A. Fukuyama, K. Nishioka, H. Suzuki, N. Kuze, Y. Moriyasu, T. Kita, A. Kotagiri, N. Kojima, A.M. Vega, M. Yamaguchi, and A.L. López, in 28th Eur. Photovolt. Sol. Energy Conf. Exhib. (2013), pp. 88–93.
5. G. Siefer, M. Steiner, M. Baudrit, C. Dominguez, I. Antón, R. Nuñez, F. Roca, P.M. Pugliatti, A.D. Stefano, R. Kenny, and P. Morabito, in AIP Conf. Proc. (AIP Publishing, 2014), pp. 167–172.
6. P. Besson, C. Domínguez, and M. Baudrit, in AIP Conf. Proc. (AIP Publishing, 2014), pp. 321–325.
7. ASTM, G173-03 Standard Tables for Reference Solar Spectral Irradiances: Direct Normal and Hemispherical on 37° Tilted Surface (ASTM International, West Conshohocken, PA, United States, 2008).
8. C. Domínguez, I. Antón, G. Sala, and S. Askins, Prog. Photovolt. Res. Appl. 21, 1478 (2013).
9. J. Jaus, T. Mißbach, S.P. Philipps, G. Siefer, and A.W. Bett, in (Http://www.black-photon.de/attachments/article/55/PVSEC_Hamburg_2011_Jaus_Component_Cells.pdf, 2011), pp. 176–181.